Diamond & Related Materials 92 (2019) 109–116

Contents lists available at ScienceDirect

Diamond & Related Materials

journal homepage: www.elsevier.com/locate/diamond

Microstructure, adhesion, in vitro corrosion resistance and tribological behavior of (Si:N)-DLC coated pure Ti

Wei Yang[a], Dapeng Xu[a], Yu Gao[a], Lin Hu[a], Peiling Ke[b,*], Jian Chen[a,*]

[a] School of Materials Science and Chemical Engineering, Xi'an Technological University, Xi'an 710032, PR China
[b] Key Laboratory of Marine New Materials and Related Technology, Zhejiang Key Laboratory of Marine Materials and Protection Technology, Ningbo Institute of Material Technology & Engineering, Chinese Academy of Sciences, Ningbo 315201, PR China

ARTICLE INFO

Keywords:
Pure Ti
(Si:N)-DLC
Interlayer
Adhesion
Microstructure and properties

ABSTRACT

(Si:N)-DLC, Si/(Si:N)-DLC, Si_3N_4/(Si:N)-DLC and Si/Si_3N_4/(Si:N)-DLC four films were deposited on the pure Ti substrates, using a hybrid ion beam deposition system consisting of a DC magnetron sputtering and linear anode-layer ion sources, to improve the adhesion and in vitro protective performance. The microstructures and thicknesses of the (Si:N)-DLC film with different interlayers were investigated by Raman spectroscopy, X-ray photoelectron spectroscopy, atomic force microscopy and scanning electron microscopy. The mechanical and adhesion properties were evaluated by indentation and scratch tests. The corrosion resistance and wear resistance of the coated pure Ti samples were characterized by electrochemical test and friction test in the SBF solution, respectively. The results showed that the (Si:N)-DLC film containing Si_3N_4 structure was obtained. This (Si:N)-DLC film interacted with the Si or Si_3N_4 interlayer, showing an obvious transition boundary, which resulted in an increasing binding force. As a result, the Si/Si_3N_4/(Si:N)-DLC film showed the highest critical loads. Furthermore, it was found that the Si/(Si:N)-DLC film had excellent in vitro corrosion resistance and tribological behavior in the SBF solution.

1. Introduction

Titanium and its alloys provide good biocompatibility and corrosion properties are commonly used as today fixation devices in orthodontics as well as in the treatment of bone traumata [1,2]. Nonetheless, these metal materials as dental and orthopedic implants are exposed to body fluid, they undergo sliding wear and corrosion [3–5]. As a result, the prolonged use of dental and orthopedic implants can result in failure due to the wear particles, as products of wear and corrosion process, leading to bone loss and loosening and failure of the implant [6]. Therefore, surface treatments have been extensively investigated for titanium implants in order to improve their properties [7–10].

Diamond-like-carbon (DLC) films have been widely used in biomedical applications due to their biocompatibility, anti-corrosion, and chemical inertness [11,12]. Many techniques, such as physical vapor deposition (PVD) and chemical vapor deposition (CVD), are being developed to deposit DLC films. More importantly, Anca Mazare et al. found that the silver doped DLC coatings exhibit an excellent antibacterial activity [13]. The F and Si doped DLC coatings can also reduce the surface energy and improved antibacterial ability of DLC coatings [14]. Especially, our previous work shows that Si and N co-doping diamond-like-carbon ((Si:N)-DLC) film has excellent mechanical and protective properties [15]. However, the poor adhesion of DLC thin films to metal substrates, as a result of high intrinsic stress, is a challenge to industrial application [16]. To resolve the failure conditions of DLC films on Ti substrates, an adhesive interlayer produced in different ways as a single- or multi-component system is used. Seokil Kang et al. report that the DLC-coated Ti-6Al-4 V with the TiCN interlayer has an excellent wear resistance due to its high hardness, elastic modulus, and interface bonding [17]. Stefan Nißen reveals that gradient Ti-a-C:H:Ti interlayer can improve a-C:H adhesion to Ti6Al4V substrates [18]. An amorphous carbon nitride (a-C:N) interlayer as a promising alternative to the amorphous Si interlayer is also deposited on Ti6Al4V substrate to improve the adhesion with DLC films [19]. M. C. Salvadori et al. discover that the formation of a broadened Si:C interface enhancing the adhesion of DLC films to the underlying silicon substrate [20]. H. Maruno and A. Nishimoto obtain that the Ti/Si-DLC multi-interlayered sample exhibits excellent mechanical and tribological Properties [21]. N. Liu et al. presents the niobium (Nb) and nitrogen (N) co-doped diamond-like carbon (DLC) film with fast apparent rate constant and low charge transfer resistance can be applied to the determination of dopamine (DA) [22].

* Corresponding authors.
E-mail addresses: kepl@nimte.ac.cn (P. Ke), chenjian@xatu.edu.cn (J. Chen).

https://doi.org/10.1016/j.diamond.2018.12.027
Received 31 October 2018; Received in revised form 25 December 2018; Accepted 30 December 2018
Available online 31 December 2018
0925-9635/

Table 1
Parameters of (Si:N)-DLC and interlayer process.

Films	Current (A)		Gas flux (sccm)			Deposition time (min)	Bias voltage (V)
	Sputtering source	Ion source	Ar	N_2	C_2H_2		
(Si:N)-DLC	1.2	0.15	70	5	10	40	−100
DLC		0.15	70			40	
Si	1.2		70			5	
Si_3N_4	1.2	0.15	70	5		5	

Table 2
Composition of SBF solution.

Order	Reagent	Amount	Container	Purity (%)
1	NaCl	8.035 g	Weighing paper	99.5
2	$NaHCO_3$	0.355 g	Weighing paper	99.5
3	KCl	0.225 g	Weighing paper	99.5
4	$K_2HPO_4{\cdot}3H_2O$	0.231 g	Weighing paper	99.0
5	$MgCl_2{\cdot}6H_2O$	0.311 g	Weighing paper	98.0
6	1.0 M·HCl	39 ml	Graduated cylinder	–
7	$CaCl_2$	0.292 g	Weighing paper	95.0
8	Na_2SO_4	0.072 g	Weighing paper	99.0
9	Tris	6.118 g	Weighing paper	99.0
10	1.0 M·HCl	0-5 ml	Syringe	–

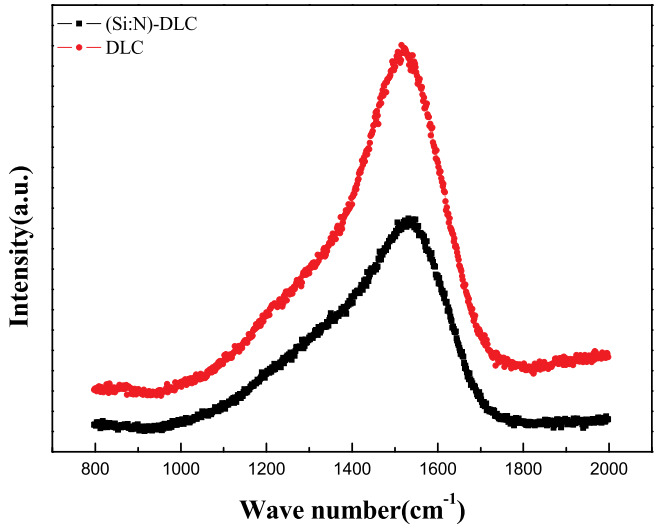

Fig. 1. Raman spectra of (Si:N)-DLC and DLC films on Si substrates.

Table 3
Details of Raman spectra for (Si:N)-DLC and DLC films.

Films	I_D/I_G	Position of G peak/(cm^{-1})
DLC	0.620	1530
(Si:N)-DLC	1.159	1544

To account for the poor adhesion and biocompatibility of DLC films for Ti substrates, the selection of interlayer should have the following characteristics: Firstly, interlayer as “buffer layers” can provide sufficient amounts of strong chemical bonds like Si—C, Ti—C, Si—N or Ti—N at the interfaces, which are particularly beneficial for adherence to metal substrates. Secondly, it is of importance to avoid abrupt mechanical or chemical changes in the interface region between two different materials, avoiding premature delamination. Thirdly, the components of interlayers do not produce biological toxicity, such as Cr and Ni inducing allergic reactions in some cases. So, in this paper, three films, such as Si monolayer, Si_3N_4 monolayer or Si/Si_3N_4 bilayer were deposited as the interlayer of (Si:N)-DLC film on the pure Ti substrate. The microstructure, adhesion, mechanical property, in vitro corrosion resistance and wear resistance in the SBF solution environment of DLC film with different chemical gradient Si, Si_3N_4 or Si/Si_3N_4 interlayer were comparatively investigated. Based on the comparison of these properties, a newly designed film/substrate system was proposed for a pure Ti substrate in this study.

2. Experimental

TA2 pure titanium specimens had a diameter of 15 mm and a thickness of 5 mm. Si specimens were cut to a size of 50 mm × 30 mm × 1 mm for the observation of cross-sectional morphologies of films. The specimens were ultrasonically cleaned in acetone and ethanol, and dried in air before being put into the vacuum chamber. The Si monolayer, Si_3N_4 monolayer or Si/Si_3N_4 bilayer as the interlayer of the (Si:N)-DLC films were deposited on the Si and TA2 pure titanium substrates by a hybrid ion beam deposition system consisting of a DC magnetron sputtering with a 120 mm (W) × 380 mm (L) rectangular Si target (99.99%) and a 380 mm (L) linear anode-layer ion sources (LIS). Prior to deposition, the substrates were sputter-cleaned for 5 min using Ar ion with a bias voltage of −100 V. The base pressure was evacuated to a vacuum of 2×10^{-5} Torr. The varied deposition process parameters for the interlayers, (Si:N)-DLC film and DLC film were shown in Table 1.

The cross-sectional morphologies and thicknesses of the four films were characterized by scanning electron microscopy (SEM). The element distribution of the wear scars of the four (Si:N)-DLC films with different interlayers after the friction test was detected by energy dispersive spectrometer (EDS). Atomic force microscopy (AFM) was performed to characterize surface morphologies of the four films. The structures of the (Si:N)-DLC film and DLC film were analyzed by Raman scattering spectroscopy in air at room temperature. The spectra were deconvoluted into D and G bands using two Gaussian curves. The intensity ratios of D and G peaks (I_D/I_G) and the shifts in the D and G bands were obtained [23]. The bonding states of the (Si:N)-DLC film were characterized by X-ray photoelectron spectroscopy (XPS) with Al (mono) Kα irradiation at pass energy of 160 eV. The binding energies were referenced to the C 1s line at 284.6 eV. The adhesion of the films to the pure Ti substrates was evaluated by a scratch tester performed on a Rockwell diamond indenter with a conical tip of 0.2 mm in radius. The normal load of the indenter was linearly ramped from the minimum value (1 N) to the maximum value (30 N) during scratching. In the test, the scratch length was 3.00 mm and the scratch speed was 1.5 mm/min. The nano-hardnesses and elasticity modulus of the four films on the top surface of the specimens were evaluated by using a nanoindentation tester with a single crystal diamond Berkovich

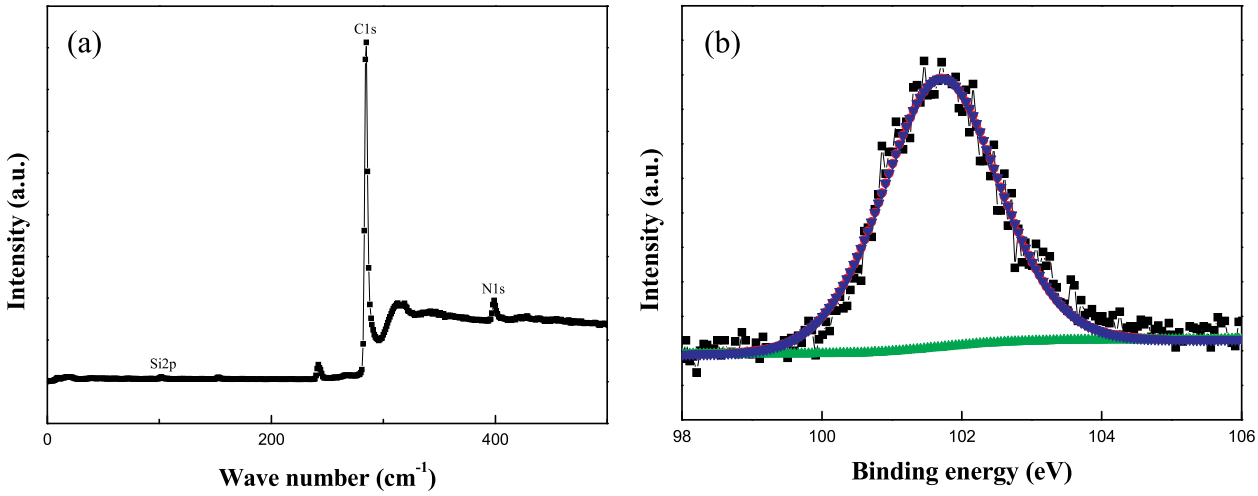

Fig. 2. (a) XPS survey spectra and (b) Si2p high resolution spectra of (Si:N)-DLC film.

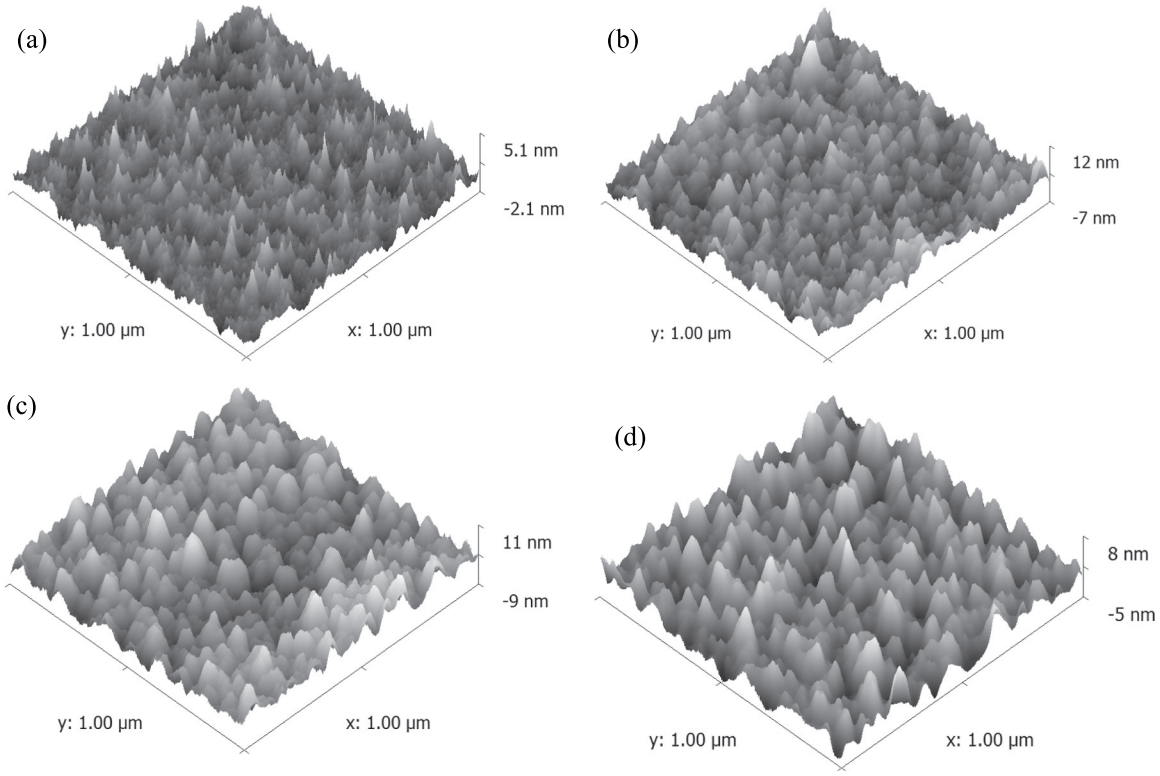

Fig. 3. AFM images of four films, (a) (Si:N)-DLC, (b) Si/(Si:N)-DLC, (c) Si_3N_4/(Si:N)-DLC and (d) Si/Si_3N_4/(Si:N)-DLC.

indenter. For each sample, more than 5 effective indentations were carried out, with the maximum indentation depths kept under the values of 10% of the total thickness for each film. The corrosion resistance of the coated pure Ti samples was evaluated by electrochemical test. All electrochemical measurements were performed at room temperature in the SBF solution. The compositions of the SBF solution were shown in Table 2. During the process of electrochemical test, a three electrode cell with the coated specimens as working electrode, the platinum sheet as auxiliary electrode, the saturated calomel electrode as the reference electrode was used. The working electrode, exposed to the electrolytic solution, was covered with a holder with a circular window having a surface area of 0.785 cm^2. Before each measurement, the open circuit potential (OCP) of samples was monitored for 5 min to stabilize the surface condition. The scanning speed was 1 mV/s. A 64 bit system-zview software was used to fit and calculate the characterization parameters of electrochemical corrosion. The tribological behaviors of the treated samples were measured on a UMT TriboLab friction tester in the SBF solution environment at room temperature. During the tests, a 2 N contact load, speed 150 mm/min and friction time 1200 s were applied on the samples against a Al_2O_3 ball. After the friction test, the wear tracks of the four films were investigated using FESEM and EDS.

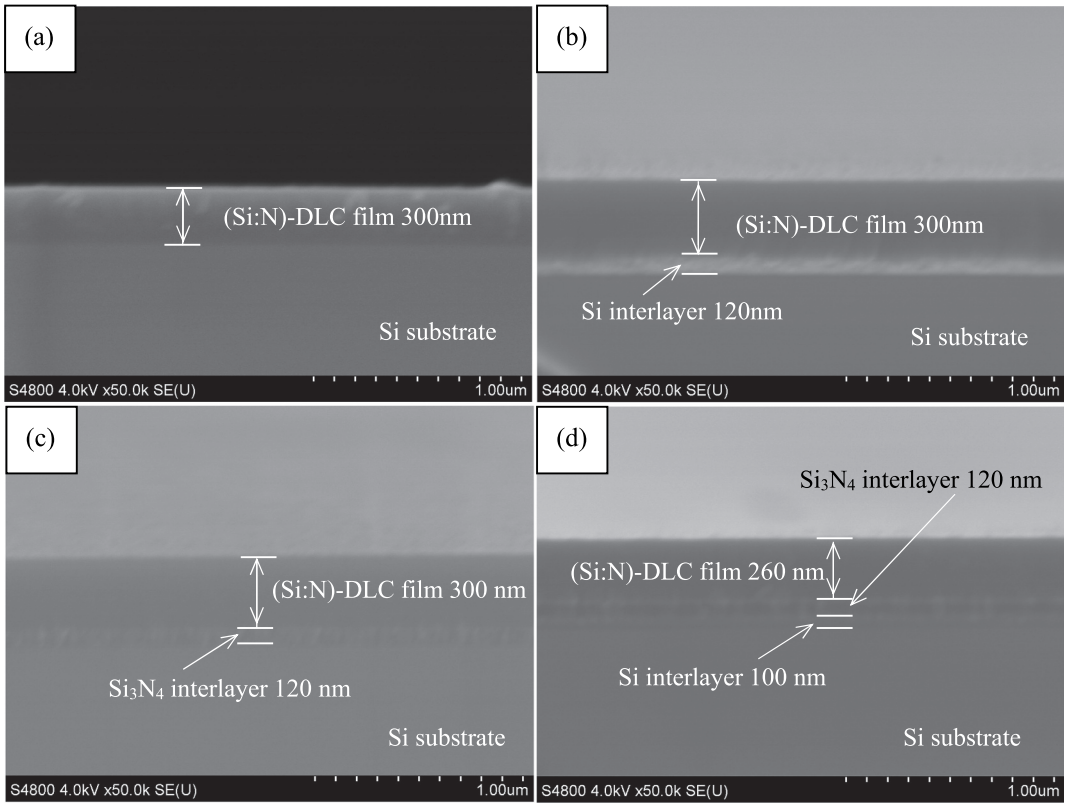

Fig. 4. Cross-sectional SEM images of four films, (a) (Si:N)-DLC, (b) Si/(Si:N)-DLC, (c) Si_3N_4/(Si:N)-DLC and (d) Si/Si_3N_4/(Si:N)-DLC.

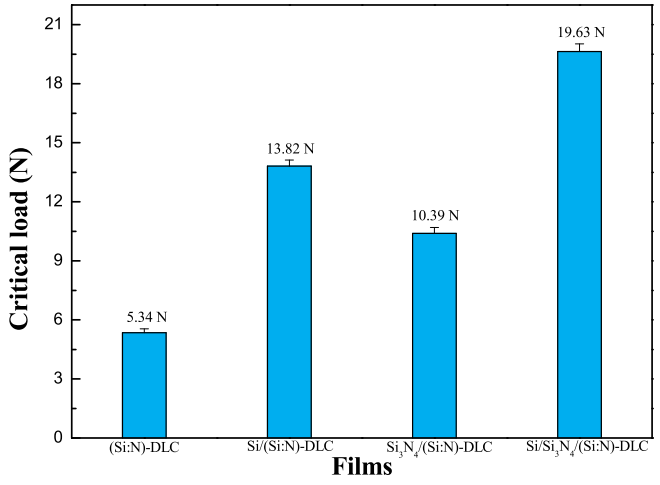

Fig. 5. Critical loads of four films on pure Ti substrates.

3. Results and discussion

Raman spectra of (Si:N)-DLC and DLC films are shown in Fig. 1 and Table 3. Usually, the Raman spectra of DLC films can be fitted using two Gaussians peaks, the G peak at approximately 1540 cm^{-1} and the D peak at approximately 1345 cm^{-1}. The G band is due to the bond stretching of all pairs of sp^2 bond in both aromatic rings and carbon chains, and D band is due to the breathing modes of sp^2 bond only in rings [24]. According to the G peak position and the intensity ratio of D peak to G peak (I_D/I_G), the sp^2/sp^3 ratio of the DLC films can be characterized [25]. In spectrum of (Si:N)-DLC film, a G peak centered at 1544 cm^{-1}. A G peak centered at 1530 cm^{-1} was found for DLC film. It is noted that the G peak position shifted towards high wave number and the I_D/I_G ratio also dramatically increased in the (Si:N)-DLC film compared with the DLC film, implying the increased sp^2/sp^3 ratio in this (Si:N)-DLC film.

As Si was an element for the carbide forming, and it also had a strong affinity with N and was easy to form a stable "network" microstructure of silicon nitride. This structure generally had superhigh hardness, excellent oxidation resistance and lubrication performance [26,27]. So the bonding natures of (Si:N)-DLC coated samples were investigated using XPS analysis. XPS survey spectra and Si2p high resolution spectra are shown in Fig. 2(a) and (b), respectively. It was found that the (Si:N)-DLC film mainly contained C, Si and N elements, and the atomic ratio of C, Si and N was 95.61%, 0.41% and 3.81%. Fig. 2(b) showed the deconvolution of Si2p peak of the (Si:N)-DLC top film, giving one peaks at 101.7 eV, which were assigned to Si_3N_4 bonds. So it could be deduced that the (Si:N)-DLC nanocomposite film containing Si_3N_4 was obtained by the designed deposition process [15].

The surface morphologies of the (Si:N)-DLC, Si/(Si:N)-DLC, Si_3N_4/(Si:N)-DLC and Si/Si_3N_4/(Si:N)-DLC four films on Ti substrates were obtained by atomic force microscopy, shown in Fig. 3. The surface roughness (Ra) of the (Si:N)-DLC, Si/(Si:N)-DLC, Si_3N_4/(Si:N)-DLC and Si/Si_3N_4/(Si:N)-DLC films was calculated as 0.51 nm, 1.67 nm, 2.05 nm and 1.58 nm, respectively. It was seen that all the four films were uniform and compact. Moreover, the surface of the DLC films was much rougher than that of DLC film without interlayer, which resulted from the matrix change of (Si:N)-DLC caused by the interlayer deposition [28].

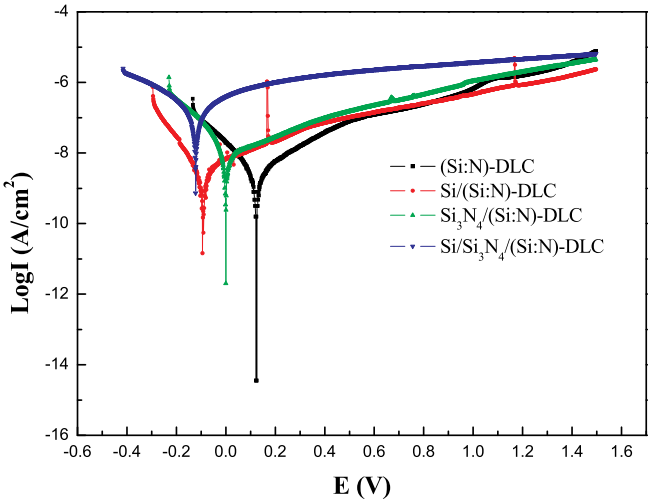

Fig. 6. Polarization curves of four coated samples in SBF solution.

Table 4
Electrochemical results obtained from the polarization curves of Fig. 6.

Film-substrate system	Corrosion current density (A/cm^2)	Corrosion potential (V)
Ti/(Si:N)-DLC	2.63×10^{-9}	0.117
Ti/Si/(Si:N)-DLC	5.43×10^{-10}	−0.091
Ti/Si_3N_4/(Si:N)-DLC	1.98×10^{-9}	−0.001
Ti/Si/Si_3N_4/(Si:N)-DLC	3.15×10^{-8}	−0.123

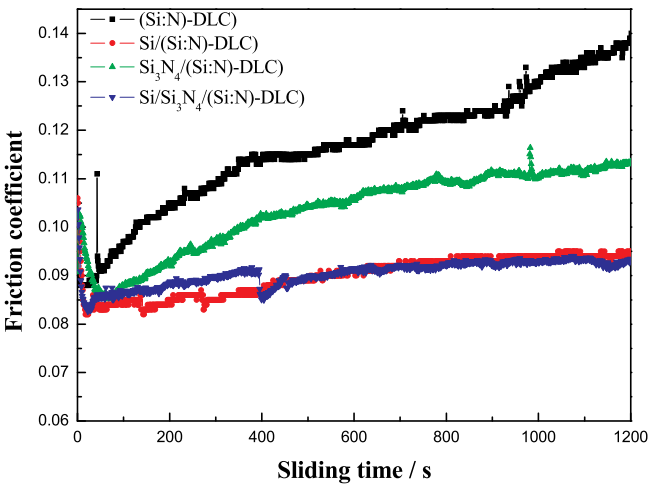

Fig. 7. Coefficient of friction (COF) of four films on Ti substrates as a function of sliding time.

Fig. 4 shows the cross-sectional SEM image of the boundary structure between the (Si:N)-DLC layer, interlayers and Si substrates. It was found that the thicknesses of the four films was approximate 300 nm, 420 nm, 420 nm and 480 nm, respectively. Actually, it was observed that the (Si:N)-DLC film interacted with the interlayer, and there was an obvious transition boundary. But the boundary between the (Si:N)-DLC monolayer and Si substrate was clear and uniform, with resulted in a poor interface integration. As a result, a suitable interlayer design was helpful to improve the binding performance of (Si:N)-DLC film with the substrate.

To obtain the high adhesion is one of the major purposes for the (Si:N)-DLC protective films on the pure Ti substrates by preparing different interlayer. Fig. 5 shows the critical loads of the four coated samples in the scratch test in this study. The results showed that all the three (Si:N)-DLC coatings with interlayer exhibited higher critical loads than the (Si:N)-DLC film without interlayer deposited on the pure Ti substrate. Especially, the Si/Si_3N_4/(Si:N)-DLC protective film showed the highest critical loads (19.63 N) among the four films due to its interface bonding microstructure and the stress release for the multilayer structure. It was believed that high bonding force was very useful to improve the tribological behavior of the coated samples.

The polarization curves of four (Si:N)-DLC coated Ti samples in the SBF solution are shown in Fig. 6. Corrosion potential and corrosion current density obtained from Fig. 6 by Tafel analysis are shown in Table 4. Based on these electrochemical parameters, the corrosion current density of Si/(Si:N)-DLC film was obviously lower than that of the other three films, indicating the best corrosion resistance among the four film-substrate. The reason might be that the corrosion resistance of the film-substrate depended on the chemical inertness of (Si:N)-DLC film and its adhesion with the substrate [29,30]. From the previous analysis, it could be found that Si/(Si:N)-DLC film had the increased adhesion with the substrate compared with the (Si:N)-DLC and Si_3N_4/(Si:N)-DLC films. However, the Si/Si_3N_4/(Si:N)-DLC film with the highest bonding force still had the highest corrosion current density, showing the worst corrosion resistance. The results of the electrochemical corrosion test were quite different from the literature, and it was found that the DLC:H/SiNx film had excellent corrosion resistance due to combination of good barrier effect of the bilayer DLC:H/SiNx film, the self-stabilized and self-sealed ability of SiNx [31]. The Si/Si_3N_4/(Si:N)-DLC film had bad corrosion resistance, which might be due to the easy formation of galvanic cell model for the complexity of the multilayer [32,33]. However, compared with the corrosion current density (4.10×10^{-11} A/cm^2) of Si-DLC film, the corrosion current density of Si/(Si:N)-DLC film was still high, which could be attributed to the formation of a dense and low-porosity coating of Si-DLC film, which impede the penetration of water and ions [34].

Fig. 7 shows the variation of the friction coefficients with the sliding time for four (Si:N)-DLC coated Ti samples against an Al2O3 ball, respectively. The Si/(Si:N)-DLC film recorded a relatively low steady-state friction coefficient of 0.085 and retained almost unchanged friction coefficient even at a sliding duration (1200 s). Although, the friction coefficient of the Si/Si_3N_4/(Si:N)-DLC film was similar with the Si/(Si:N)-DLC film after 400 s sliding duration, it sharply decreased to about 0.85 from 0.9 at 400 s, indicating a different friction behavior. Under the same testing condition, the friction coefficients of (Si:N)-DLC monolayer and Si_3N_4/(Si:N)-DLC film increased significantly with the increase of sliding time, and the friction coefficients of (Si:N)-DLC and Si_3N_4/(Si:N)-DLC films were close to 0.14 and 0.11 after 1200 s wear, respectively. Thus, it could be obtained that the (Si:N)-DLC films with the suitable interlayer on the Ti substrates had excellent friction-reduction and wear resistance behavior.

To investigate the tribological behavior of the obtained films on the Ti substrate, the SEM morphologies of the wear scar are shown in Fig. 8 and the partially elaborated chemical composition by EDS is shown in Table 5. The results showed that the width of wear scars of the (Si:N)-DLC, Si/(Si:N)-DLC, Si_3N_4/(Si:N)-DLC and Si/Si_3N_4/(Si:N)-DLC four films was 322.5 μm, 150.1 μm, 246.8 μm, and 212.1 μm, respectively. It was observed that the wear scar of (Si:N)-DLC coated Ti substrate was broad and deep. Some abrasive grains were found in the wear scar, resulting in the increasing friction coefficient with sliding time, which presented the features of adhesive wear. In the case of Si_3N_4/(Si:N)-DLC film, the wear scar was broad but not deep, presenting furrow wear characteristic. For the Si/(Si:N)-DLC and Si/Si_3N_4/(Si:N)-DLC two films, their wear scar

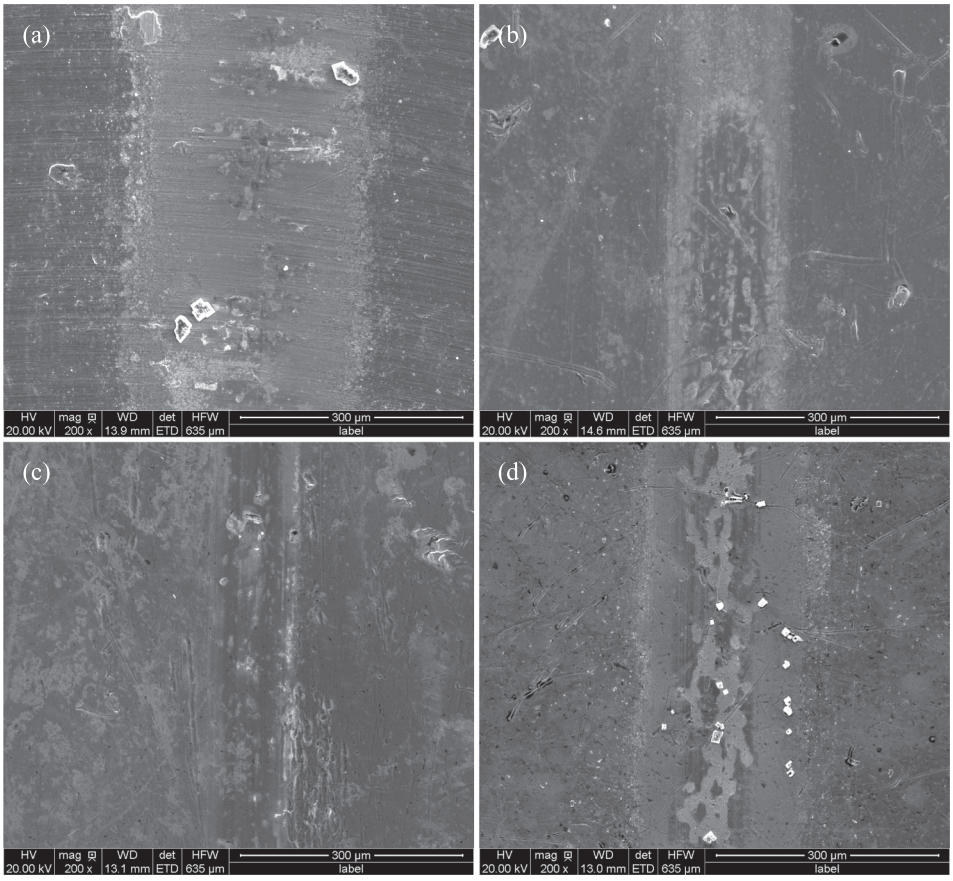

Fig. 8. SEM morphologies of four films after friction tests, (a) (Si:N)-DLC, (b) Si/(Si:N)-DLC, (c) Si_3N_4/(Si:N)-DLC and (d) Si/Si_3N_4/(Si:N)-DLC.

Table 5
Composition at wear tracks of four films in Fig. 8.

Films	C	N	O	Al	Si	Ti
(Si:N)-DLC	62.89	0.35	3.07	0.14	0.09	33.46
Si/(Si:N)-DLC	65.00	1.38	3.17	0.09	2.73	27.63
Si_3N_4/(Si:N)-DLC	64.71	2.53	3.66	0.01	1.52	28.04
Si/Si_3N_4/(Si:N)-DLC	57.83	0.30	8.37	0.09	2.86	30.54

width was relatively small, showing slight adhesive wear. It was interesting that some local regions of the top (Si:N)-DLC film had been stripped from the Si/Si_3N_4/(Si:N)-DLC film, but it still showed small the friction coefficient. Also, it was discovered that the friction coefficient decreased significantly at 400 s sliding, which might be attributed to the C peeled from the Si/Si_3N_4/(Si:N)-DLC film played a good lubrication role at the friction interface. Generally, a large number of C were detected from the wear trace of the four coated substrates, indicating that the (Si:N)-DLC film still survived. It was also confirmed that a little of O was found from the wear trace of the four (Si:N)-DLC coated samples. This revealed that the formation of oxide due to the temperature spikes between the counter-body steel ball and the film during the friction was strongly restrained for the lubrication of carbon film [35]. In conclusion, the (Si:N)-DLC films with different interlayer could greatly improve the wear resistance of the Ti substrates in this study.

Raman spectra, I_D/I_G values and position of G peak of (Si:N)-DLC films with different interlayers before and after friction tests are shown in Fig. 9 and Table 6, respectively. It was found that the G peak of (Si:N)-DLC, Si/(Si:N)-DLC and Si_3N_4/(Si:N)-DLC films slightly shifted to the right after wear, but it slightly shifted to the left after wear for the Si/Si_3N_4/(Si:N)-DLC film. Compared with the four (Si:N)-DLC films with different interlayers before wear, the I_D/I_G value for the (Si:N)-DLC film without interlayer significantly decreased and the I_D/I_G value for Si/Si_3N_4/(Si:N)-DLC and Si_3N_4/(Si:N)-DLC films slightly reduced after friction test, indicating the increased sp^2/sp^3 ratio and enhanced graphitization. This result also revealed that the high temperature oxidation phenomenon was obvious during the friction process. For the Si/(Si:N)-DLC film, its I_D/I_G value increased after friction test, indicating an enhanced degree of diamond. It indicated that the high temperature oxidation phenomenon was effectively suppressed during friction process, showing an excellent wear resistance. This result was consistent with the results of friction curve and the analysis of wear scar.

4. Conclusions

1) The (Si:N)-DLC film with Si_3N_4 phase was obtained by using a hybrid ion beam deposition system consisting of a DC magnetron sputtering and linear anode-layer ion sources. The Si/Si_3N_4/(Si:N)-DLC protective film formed an obvious transition boundary showed the highest critical loads (19.63 N).
2) The Si/(Si:N)-DLC film showed an excellent corrosion resistance in the SBF solution for its increased adhesion with the substrate, and the corrosion current density of this film was 5.43×10^{-10} A/cm^2. But the Si/Si_3N_4/(Si:N)-DLC film with highest bonding force (19.63 N) had the worst corrosion resistance (3.15×10^{-8} A/cm^2) due to a formation of galvanic cell model for the complexity of the multilayer.

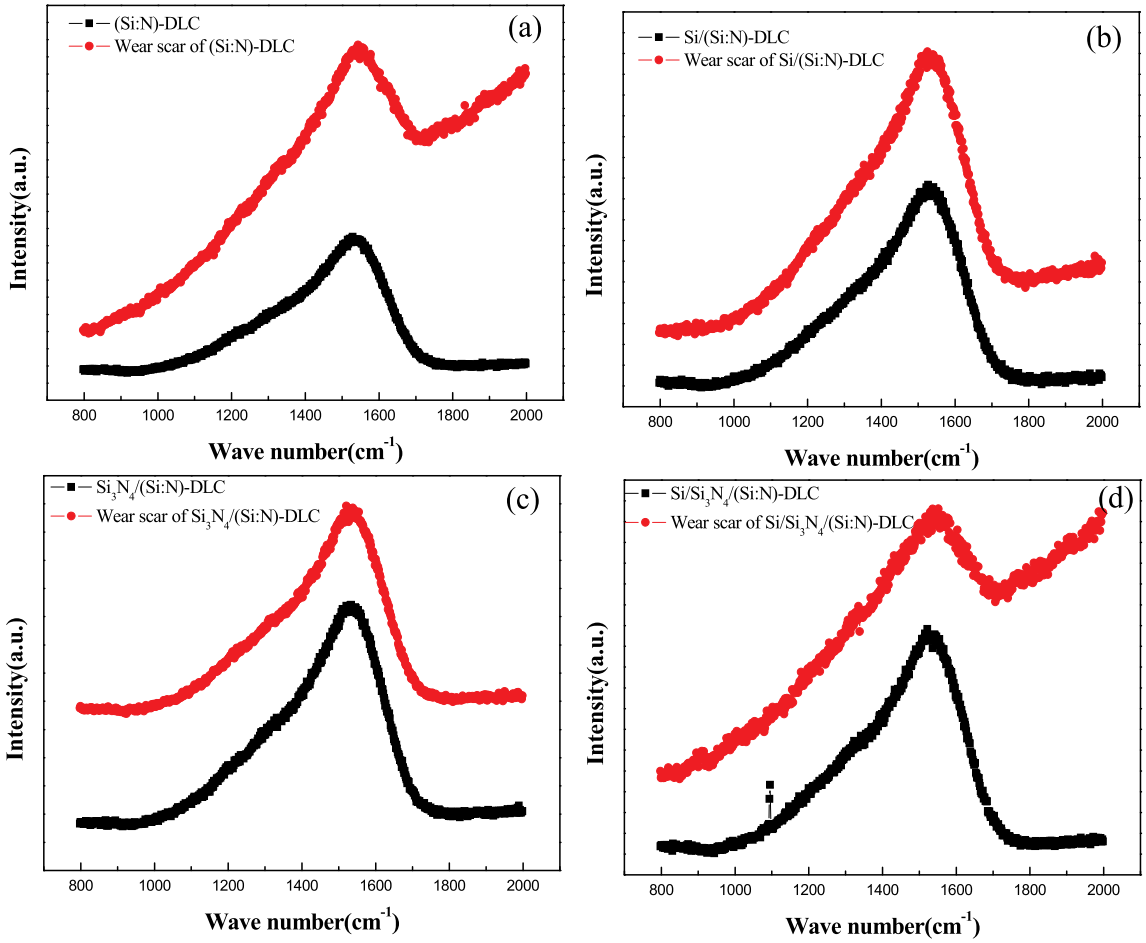

Fig. 9. Raman spectra of four films before and after friction tests, (a) (Si:N)-DLC, (b) Si/(Si:N)-DLC, (c) Si_3N_4/(Si:N)-DLC and (d) Si/Si_3N_4/(Si:N)-DLC.

Table 6
Raman analysis results of four films before and after friction tests.

Films	I_D/I_G	Position of G peak
(Si:N)-DLC	1.77	1544.59
Wear scar of (Si:N)-DLC	1.01	1545.72
Si/(Si:N)-DLC	1.16	1544.12
Wear scar of Si/(Si:N)-DLC	1.29	1545.78
Si_3N_4/(Si:N)-DLC	1.11	1544.59
Wear scar of Si_3N_4/(Si:N)-DLC	1.06	1545.55
Si/Si_3N_4/(Si:N)-DLC	1.14	1543.68
Wear scar of Si/Si_3N_4/(Si:N)-DLC	1.08	1539.6

3) The Si/(Si:N)-DLC film had the lowest friction coefficient (about 0.087) and wear scar width (150.1 μm) in the SBF solution. For the application of functional (Si:N)-DLC films deposited on medical Ti and its alloy, the traditional Si interlayer was a prior selection.

Acknowledgment

The authors gratefully acknowledge the financial support of the Natural Science Foundation of China (Grant No. 51471123), the Key Research and Development Plan of Shaanxi Province - Industrial Project (Grant No. 2018GY-127) and Shaanxi Provincial Education Department Program (18JK0394). The authors would like to express their special thanks to Nan Li (at School of Materials Science and Chemical Engineering, Xi'an Technological University) for their help in characterization of films for this paper.

References

[1] H.S. Baumgarten, 5.1: why titanium in dental applications? Titanium in Medical and Dental Applications, 2018, pp. 495–504.
[2] A.H. Hussein, Mohamed A.H. Gepreel, M.K. Gouda, Ahmad M. Hefnawy, Sherif H. Kandil, Biocompatibility of new Ti–Nb–Ta base alloys, Mater. Sci. Eng. C 61 (2016) 574–578.
[3] W. Xu, X. Lu, L.N. Wang, Z.M. Shi, S.M. Lv, M. Qian, X.H. Qu, Mechanical properties, in vitro corrosion resistance and biocompatibility of metal injection molded Ti-12Mo alloy for dental applications, J. Mech. Behav. Biomed. Mater. 88 (2018) 534–547.
[4] Y. Huang, H.J. Zeng, X.X. Wang, D.S. Wang, Corrosion resistance and biocompatibility of SrHAp/ZnO composite implant coating on titanium, Appl. Surf. Sci. 290 (2014) 353–358.
[5] Y. Wang, H.J. Yu, C.Z. Chen, Z.H. Zhao, Review of the biocompatibility of micro-arc oxidation coated titanium alloys, Mater. Des. 85 (2015) 640–652.
[6] N.S. Manam, W.S.W. Harun, D.N.A. Shri, S.A.C. Ghani, T. Kurniawan, M.H. Ismail, M.H.I. Ibrahim, Study of corrosion in biocompatible metals for implants: a review, J. Alloys Compd. 701 (2017) 698–715.
[7] J.W. Lu, Y. Zhang, W.T. Huo, W. Zhang, Y.Q. Zhao, Y.S. Zhang, Electrochemical corrosion characteristics and biocompatibility of nanostructured titanium for implants, Appl. Surf. Sci. 434 (2018) 63–72.
[8] M.M. Hatamleh, X.L. Wu, A. Alnazzawi, J. Watson, D. Watts, Surface characteristics and biocompatibility of cranioplasty titanium implants following different surface treatments, Dent. Mater. 34 (2018) 676–683.
[9] W. Yang, D.P. Xu, Q.Q. Guo, T. Chen, J. Chen, Influence of electrolyte composition on microstructure and properties of coatings formed on pure Ti substrate by micro arc oxidation, Surf. Coat. Technol. 349 (2018) 522–528.
[10] B. Szaraniec, K. Pielichowska, E. Pac, E. Menaszek, Multifunctional polymer coatings for titanium implants, Mater. Sci. Eng. C 93 (2018) 950–957.
[11] L. Mohan, C. Anandan, V.K. William Grips, Corrosion behavior of titanium alloy Beta-21S coated with diamond like carbon in Hank's solution, Appl. Surf. Sci. 258 (2012) 6331–6340.
[12] J.L. Lin, X.H. Zhang, P. Lee, R.H. Wei, Thick diamond like carbon coatings deposited by deep oscillation magnetron sputtering, Surf. Coat. Technol. 315 (2017) 294–302.
[13] A. Mazare, A. Anghel, C. Surdu-Bob, G. Totea, I. Demetrescu, D. Ionita, Silver doped

diamond-like carbon antibacterial and corrosion resistance coatings on titanium, Thin Solid Films 657 (2018) 16–23.
[14] D.W. Ren, Q. Zhao, A. Bendavid, Anti-bacterial property of Si and F doped diamond-like carbon coatings, Surf. Coat. Technol. 226 (2013) 1–6.
[15] W. Yang, Z.N. Deng, D. Zhang, P.L. Ke, A.Y. Wang, Microstructure and tribological behavior of self-lubricating (Si:N)-DLC/MAO coatings on AZ80 magnesium substrate, Acta Metall. Sin. (Engl. Lett.) 26 (2013) 693–698.
[16] A.Y. Wang, H.S. Ahn, K.R. Lee, J.P. Ahn, Unusual stress behavior in W-incorporated hydrogenated amorphous carbon films, Appl. Phys. Lett. 86 (2005) 2740–2743.
[17] S. Kang, H.P. Lim, K. Lee, Effects of TiCN interlayer on bonding characteristics and mechanical properties of DLC-coated Ti-6Al-4V ELI alloy, Int. J. Refract. Met. Hard Mater. 53 (2015) 13–16.
[18] S. Nißen, J. Heeg, M. Warkentin, D. Behrend, Marion Wienecke, The effect of deposition parameters on structure, mechanical and adhesion properties of a-C:H on Ti6Al4V with gradient Ti-a-C:H:Ti interlayer, Surf. Coat. Technol. 316 (2017) 180–189.
[19] C.C. Chou, J.S. Lin, R. Wu, Microstructures and mechanical properties of an a-C:N film as the interlayer and the outmost layer of a DLC-deposited Ti bio-alloy, Ceram. Int. 43 (2017) S776–S783.
[20] M.C. Salvadori, F.S. Teixeira, W.W.R. Araújo, L.G. Sgubin, I.G. Brown, Interface tailoring for adhesion enhancement of diamond-like carbon thin films, Diam. Relat. Mater. 25 (2012) 8–12.
[21] H. Maruno, A. Nishimoto, Adhesion and durability of multi-interlayered diamond-like carbon films deposited on aluminum alloy, Surf. Coat. Technol. 354 (2018) 134–144.
[22] N. Liu, H.K. Zhu, Q.P. Wei, H.Y. Long, Z.J. Deng, Z.M. Yu, Y.N. Xie, A niobium and nitrogen co-doped DLC film electrode and its electrochemical properties, J. Electrochem. Soc. 164 (2017) H1091–H1098.
[23] W.G. Cui, Q.B. Lai, L. Zhang, F.M. Wang, Quantitative measurements of sp^3 content in DLC films with Raman spectroscopy, Surf. Coat. Technol. 205 (2010) 1995–1999.
[24] A. Ferrari, J. Robertson, Interpretation of Raman spectra of disordered and amorphous carbon, Phys. Rev. B 61 (2000) 14095–14107.
[25] J. Robertson, Diamond-like amorphous carbon, Mater. Sci. Eng. R 37 (2002) 129–281.
[26] J.J. Liu, J. Yang, Y. Yu, Q.C. Sun, Z.H. Qiao, W.M. Liu, Self-lubricating Si_3N_4-based composites toughened by in situ formation of silver, Ceram. Int. 44 (2018) 14327–14334.
[27] J.J. Yu, W.M. Guo, W.X. Wei, H.T. Lin, C.Y. Wang, Fabrication and wear behaviors of graded Si_3N_4 ceramics by the combination of two-step sintering and β-Si_3N_4 seeds, J. Eur. Ceram. Soc. 38 (2018) 3457–3462.
[28] S. Mordo, V. Popravko, A. Barari, Study of the effect of coating parameters and substrates on 3D surface roughness in diamond-like-carbon coating process, IFAC Proc. Vol. 46 (2013) 1861–1866.
[29] W. Yang, Y.C. Guo, D.P. Xu, J.H. Li, P. Wang, P.L. Ke, A.Y. Wang, Microstructure and properties of (Cr:N)-DLC films deposited by a hybrid beam technique, Surf. Coat. Technol. 261 (2015) 398–403.
[30] C.J. Wang, B.L. Jiang, M. Liu, Y.F. Ge, Corrosion characterization of micro-arc oxidization composite electrophoretic coating on AZ31B magnesium alloy, J. Alloys Compd. 621 (2015) 53–61.
[31] H.K. Zhu, T. Zhao, Q.P. Wei, N. Liu, L. Ma, Z.Q. Hu, Y.J. Wang, Z.M. Yu, Corrosion resistance improvement of Mg alloy AZ31 by combining bilayer amorphous DLC:H/SiN_x film with N^+ ions implantation, J. Alloys Compd. 762 (2018) 171–183.
[32] Y.Y. Cheng, X.L. Pang, K.W. Gao, H.S. Yang, A.A. Volinsky, Corrosion resistance and friction of sintered NdFeB coated with Ti/TiN multilayers, Thin Solid Films 550 (2014) 428–434.
[33] P.A. Schweitzer, Fundamentals of Corosion Mechanisms, Causes, and Preventative Methods, CRC press, 2010, pp. 41–43.
[34] H.G. Kim, S.H. Ahn, J.G. Kim, S.J. Park, K.R. Lee, Corrosion performance of diamond-like carbon (DLC)-coated Ti alloy in the simulated body fluid environment, Diam. Relat. Mater. 14 (2005) 35–41.
[35] Y. Liu, A. Erdemir, E.I. Meletis, A study of the wear mechanism of diamond-like carbon films, Surf. Coat. Technol. 82 (1996) 48–56.